Simulation Design of Muscle Robotic Arm Controller Based on EPC Feedforward

Shuo Jiao

School of Electrical & Information Engineering, Northeast Petroleum University, Daqing, 150000, China
fgnxfng523@gmail.com

Abstract. Coupled nonlinear muscle control and non-tracking control have become key research focuses in recent years as effective control solutions for coupled nonlinear systems. Equilibrium Point Control (EPC) as a non-tracking controller based on Particle balance theory has a wide range of application prospects. Based on parameters from real experiments, a simulation model is constructed using the MuJoCo engine, and the Generalized State Control (GSC) is introduced to mitigate the bias inherent in EPC. To mitigate the end-effector oscillation issue associated with traditional EPC controllers, a model-based motion variable feedback approach was introduced, significantly enhancing the performance of the EPC. Finally, a solution was proposed to reduce the model instability caused by the introduction of feedback. Experimental results indicate that the improved Feedback EPC (FEPC) significantly outperforms the original approach in the simulated muscle model. However, the introduction of feedback causes the model to become unstable under GSC. Consequently, it is necessary to design a suitable segmented control scheme tailored to specific control requirements. Through in-depth research, the improved FEPC is expected to become a superior enhancement to the traditional EPC control scheme.

Keywords: EPC Controller, Mujoco Engine Simulation, Bionic Muscle Model

1 Introduction

In recent years, Bio-inspired actuators have become an important research direction in robotics and bioengineering fields. Different from traditional force-generating actuators, bio-inspired actuators exhibit a high power-to-weight ratio, inherent compliance, and a wide range of motion. This allows them to operate without the need for complex linkage designs or other cumbersome mechanisms [1]. Muscle actuators also have a higher strength-to-weight ratio while also providing an expanded solution space [2].

However, the control of coupled nonlinear muscle systems has always been a challenge. The nonlinear characteristics of bio-inspired actuators make the design of control strategies more complex. Currently, the most common approach to address this issue is to reduce nonlinear deviations by designing adaptive stiffness controllers [3]. Another solution is to leverage the decoupling characteristics to mitigate the effects of

J. Iqbal (ed.), *Proceedings of the 2025 2nd International Conference on Mechanics, Electronics Engineering and Automation (ICMEEA 2025)*, Advances in Engineering Research 272,
https://doi.org/10.2991/978-94-6463-821-9_23

coupling by employing methods such as Active Disturbance Rejection Control (ADRC) controllers [4]. Regulating based on material characteristics is also a viable solution. This regulation is achieved through a self-sensing control method for AMM muscles [5]. Furthermore, data-driven control strategies also garnered increasing attention. By utilizing gradients in neural networks to construct a linearized discrete state-space representation, precise control of joints can be achieved even in the absence of a known model [6].

Although these control methods perform well in accuracy, most of them employ trajectory-based control. While this enhances control precision, it also requires extensive computations during the control process. Relative to trajectory-based control, non-trajectory control addresses this issue by calculating only the target points. This makes them provide stronger resistance to disturbances in complex system structures. The Theory of particle equilibrium is an important research direction in non-trajectory control. It focuses on the mechanical equilibrium among various particles in the system. By analyzing the interactions and motion states of the particles, reliable control strategies can be designed by utilizing physical modeling.

The Equilibrium Point Controller (EPC) is a non-trajectory control strategy based on the particle balance theory [7]. It models the skeletal and muscular systems to predict the state of the endpoint. The predict result will used as a feedforward value input. This approach maintains good robustness against disturbances even in the presence of complex model structures. But the EPC controller itself can't eliminate deviations. Although the control process is rapid, it will always experience discrepancies due to the gap between reality and the model. Besides, the control strategy inherently leads to endpoint oscillation issues.

This paper aims to investigate the shortcomings of the EPC controller and propose improvements for the potential deficiencies. First, the muscle simulation model is constructed based on Thelen muscle model, and the skeletal dynamics model is established using the known physical EPC controller [8]. Next, the EPC-GSC controller is designed based on this model. Finally, feasible improvement proposals are put forward in response to the control results of the EPC controller.

2 Data and Method

2.1 Experimental Environment and Data Sources

To achieve the design and improvement of the EPC algorithm controller, the MuJoCo engine can be used as a physical simulation platform. The MuJoCo engine itself provides muscle actuators; however, considering that their parameters are not definable, this paper develops a muscle simulation function in Python to serve as a muscle model.

The operation flow of the entire simulation system is illustrated in Fig. 1. The muscle model exists as an actuator within the MuJoCo engine, where the physical simulation is carried out by MuJoCo. The controller outputs activation values by collecting the computation results from the engine, with these activation values serving as inputs to activate the muscles and exert control.

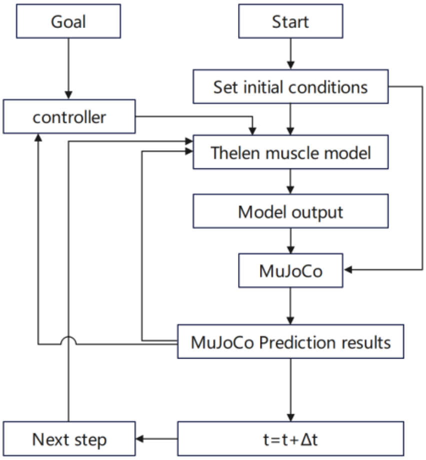

Fig. 1. Overview of the Simulation Model Workflow(Picture credit : Original)

2.2 Construction of the Muscle Model and Skeletal Model

The muscle model is the core component of the entire simulation model. The choice of the Thelen muscle model is due to its improvement on the Hill-type model, which requires fewer parameter settings and offers high biological accuracy. Therefore, it can effectively simulate the mechanical properties of muscles.

According to the Thelen muscle model, the muscle structure, from a macroscopic perspective, consists of two components: tendons and muscle fibers. Tendons do not generate force but serve a traction role. Muscle fibers are responsible for generating contraction force. Through the contraction of the muscle fibers, the tendons are elongated. This can induce tension and subsequently drive the mechanical structure to produce movement. In the Thelen model, the tendon force calculation formula is provided in Equation (1).

Although the magnitude of the force remains linear with respect to elongation beyond the segment point, the estimation of tendon strain may become inaccurate at strains reaching 3% if stress cannot be measured [9]. Therefore, this study utilizes only the linear portion of the tendon force, ensuring that the elongation remains consistent with the linear characteristics of tension by maintaining the muscle force above the value $\boldsymbol{\varepsilon}^{\mathrm{T}}$. In this model, the tensile strength of the tendon material is selected based on the linear function of the tendon, with a value of 1.2 GPa.

$$f^{TD} = F^{TD}/F_0^M = \begin{cases} f_{toe}^T \cdot (e^{k_{toe}(\varepsilon^T/\varepsilon_{toe}^T)} - 1)/(e^{k_{toe}} - 1) & \varepsilon^T < \varepsilon_{toe}^T \\ k_{lin}(\varepsilon^T - \varepsilon_{toe}^T) + f_{toe}^T & \varepsilon^T \geq \varepsilon_{toe}^T \end{cases} \quad (1)$$

The muscle fiber force consists of two components: the active contraction force $\mathrm{F^{CE}}$ and the passive stretching force $\mathrm{F^{PE}}$. $\mathrm{F^{CE}}$ is the primary force output of the muscle, which is controlled by activation signals. $\mathrm{F^{PE}}$ arises only when the muscle fibers are excessively stretched. Furthermore, the active contraction force is related to the length of the muscle fibers, denoted as $\mathrm{f_l}$. The rate of muscle fiber contraction is denoted as $\mathrm{f_v}$. Parameters $\varepsilon_0^{\mathrm{m}}$ and $\mathrm{k^{PE}}$ are model settings, while $\mathrm{f^{PE}}$ is solely related to the muscle fiber length $\mathrm{l^m}$. For the control signals of the muscles, the activation of the signals is an accumulative process. Referencing the single stimulus contraction response curve in neurobiology, τ_{act} is set to 50ms and τ_{dact} to 100ms to approximate the delay in neural response time [10]. The remaining variables are provided as fixed parameters in the referenced literature. To aid readers in clarifying the relationships among the variables and parameters, the diagram illustrating the model's formula variables is presented in Fig. 2. Parameters t_c, k^{PE}, ε_0^m, A_f, F_{len}^M, γrepresent the general parameters of the Thelen model, while parameters L_s^t, F_0^m, t_c, α, L_0^M correspond to the parameters of the reproduced muscle model.From the relationship among the parameters, it is evident that the muscle's output force is a function of the muscle activation value, the contraction velocity of the muscle fibers, and the length of the muscle fibers. Therefore, by collecting and inputting these three values, the simulated output value of the muscle can be obtained.

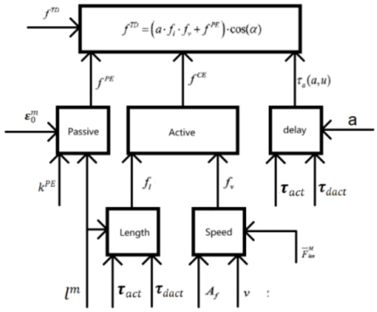

Fig. 2. Relationship Diagram of Muscle Model Parameters(Picture credit : Original)

Muscles serve as the actuators of the system, but they require the skeletal structure to generate movement. To facilitate the reproduction of control behaviors, the skeletal structure and parameters will reference the literature. It can be enhancing the accuracy of the simulation. Then, a MuJoCo physical structure can created with this skeletal mechanics model. It will serve as the model predictive component of the EPC controller. The model structure is illustrated in Fig. 3.

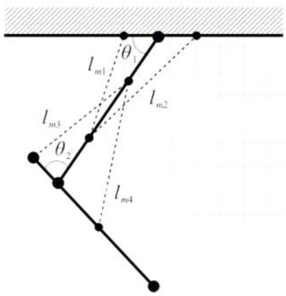

Fig. 3. Simplified Diagram of the Musculoskeletal Arm(Picture credit : Original)

2.3 Algorithm Establishment

By utilizing a simulation environment, the control algorithm can be simulated. Fig. 4 shows The traditional EPC controller. EPC controller takes the target angle and the activation value of the passive muscle as inputs. By using the structure of the equilibrium point's position, it predicts the muscle force required for the target position. Through the inverse function of the model, the activation value for the predicted target position is obtained. Finally, the control muscle activation value predicted is used as a feedforward variable input, which achieves the endpoint prediction of the target activation value.

From the perspective of control theory, the EPC controller directly computes the final value, which highly reduces the calculation. The output signal based on the endpoint target exhibits strong anti-interference capabilities. But EPC controller cannot mitigate errors. So, it’s necessary to introduce an additional control algorithm to eliminate steady-state errors. This paper will use GSC to achieve this.

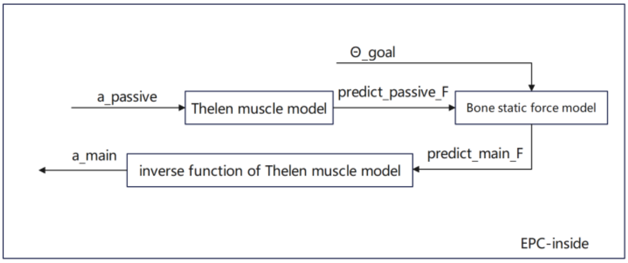

Fig. 4. Internal Schematic of the EPC Balancing Predictor(Picture credit : Original)

3 Results Analysis

3.1 Modeling Analysis

Using the simulation function of the Thelen muscle model, the solution space of the muscle model is illustrated in Fig. 5 a). The velocity V, activation value a, and muscle length L are all variables that influence muscle tension. The planar solution for a muscle force of 120 N is shown in Fig. 5 b). At the same force, the solutions for the muscle form a plane, which represents the high degree of freedom characteristic of the biomimetic muscle.

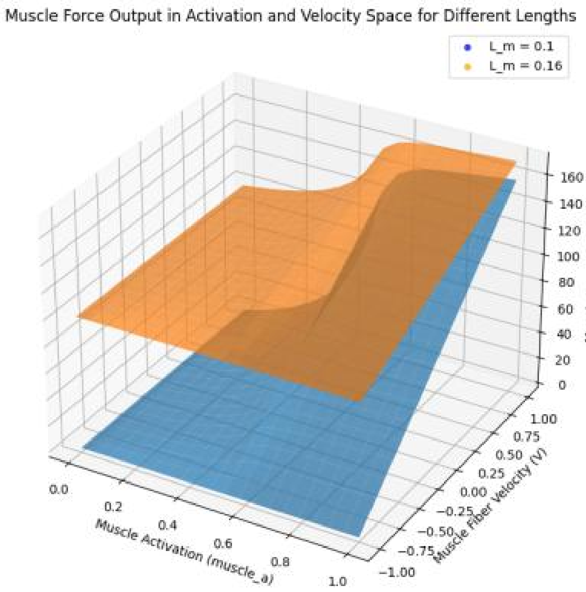

a

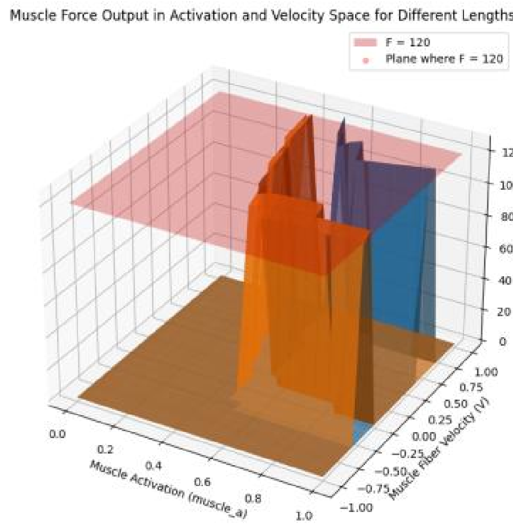

b

Fig. 5. (a) Global Solution Space of the Muscle Model, (b) Solution Space under a Force Balance of 120 N(Picture credit : Original)

The skeletal structure is established based on the parameters from the paper (Fig. 6 (a)). However, since the muscle is approximated as a spring, the absence of damping between muscle joints can lead to oscillation phenomena (Fig. 6 (b)). Therefore, an additional friction loss of 0.1 N needs to be introduced in the skeletal joint section to compensate for the discrepancies with the real environment.

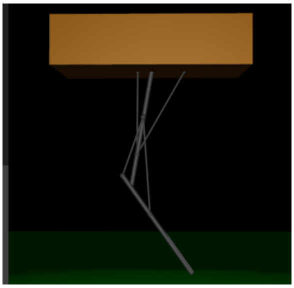

a

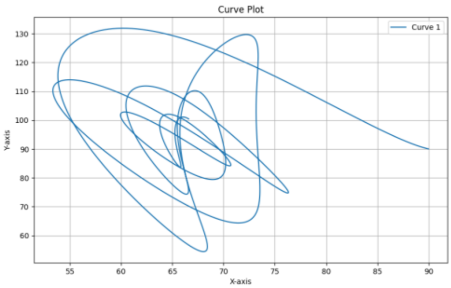

b

Fig. 6. (a) Skeletal model of the simulation platform, (b) Terminal oscillation without friction loss(Picture credit : Original)

3.2 Analysis of the EPC-GSC Feedforward Controller

Compared to trajectory control, the EPC controller has a smaller computational load and faster control speed, but it cannot eliminate steady-state error. Although the GSC controller performs well in terms of control effectiveness, the inherent nonlinear characteristics of the muscles lead to variations in its transfer function under different load conditions. This means that the optimal control parameters for the model in one state may not be optimal in another state and may even result in significant control deviations. Therefore, the EPC-GSC controller can be utilized, where EPC is responsible for predicting the target control endpoint, while GSC is tasked with eliminating steady-state error, effectively compensating for each other's shortcomings.

Table 1. Deviation Suppression Parameters under EPC Feedforward

Global Gain	0.00000012	Kp	Ki	Kd
Large Error	e> 5.0°	2.1	1.1	0.0085
Medium Error	e> 1°	3.9	0.8	0.0085
Small Error	e<=1°	4.2	0.2	0.0085

The operating performance of the EPC-GSC feedforward controller under the parameters in Table 1 is shown in Fig. 7.

The results indicate that when only using EPC, the output activation value becomes a step function. Therefore, its control accuracy will entirely depend on the accuracy of the predictive model.

With the introduction of GSC, the system can approach the target point. The control effect generated by GSC is shown in Fig. 7 (b).

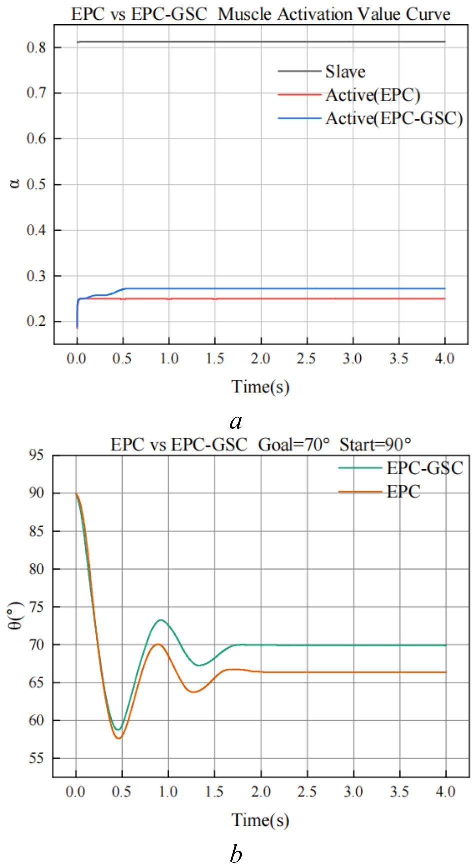

Fig. 7. (a) Angle Variation Curve, (b) Activation Values of Primary and Secondary Muscles(Picture credit : Original)

To ensure that the EPC-GSC maintains sufficient accuracy under different deviations, GSC is configured to increase the control gain only when approaching the steady state, based on the control characteristics of EPC. The control effect under this control logic is illustrated by the orange curve in Fig. 8, which represents the GSC controller eliminating steady-state deviation when the deviation is below a certain threshold, stabilizing the system at 75°. The green curve represents the control effect without this control logic; although the deviation displacement is reduced to 2/3, the control system exhibits a higher steady-state error under this configuration.

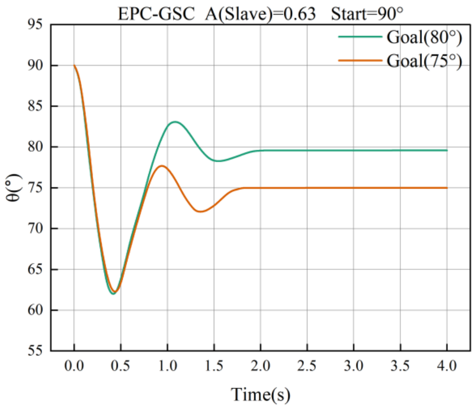

Fig. 8. illustrates the control effect under the EPC-GSC feedforward configuration.(Picture credit : Original)

However, despite this control method's ability to mitigate the deviations caused by coupling, it inherits the shortcomings of PID control. An inappropriate D parameter can easily lead to instability in control (as shown in Fig. 9): when the integral is too small, it cannot eliminate steady-state error (D = 0.0002), while an excessively large integral can cause instability in the control results over extended periods (D = 0.02). Therefore, when using this control method, the selection of the D parameter needs to be based on the real model.

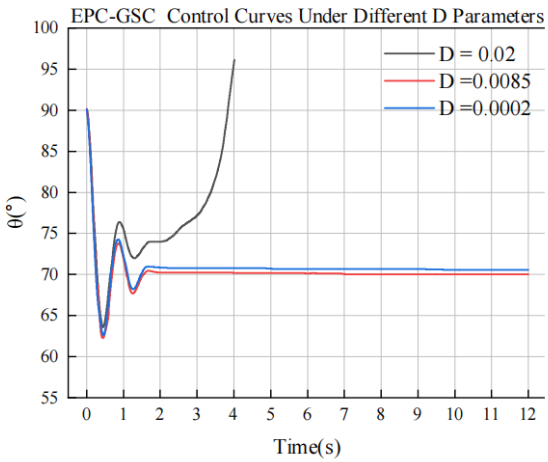

Fig. 9. illustrates the impact of the D parameter on control performance under the EPC-GSC feedforward configuration.(Picture credit : Original)

3.3 Improvements to the Feedforward Controller Based on EPC-GSC

This paper introduces the EPC feedforward controller building on the GSC. It can mitigate the impact of the muscle's coupled nonlinear characteristics on control accuracy. However, the motion of the muscle model still demonstrates oscillatory behavior after the control signal is generated. Most existing studies address this issue by increasing structural damping or ignoring the oscillations. In fact, introducing a feedback variable based on muscle length is also a solution. This paper proposes an improved EPC (FEPC) control strategy, which is expected to effectively reduce oscillations and enhance control accuracy. Since the force generated by the muscle arises from two components—the force from the activation signal and the passive tension from elongation—the muscle can be approximated as a spring to some extent. The maximum force of a spring is related to its length, and the force generated by excessive stretching is also related to the muscle length in conjunction with the active activation force. If muscle fiber length can be incorporated as a feedback variable in the EPC controller, it may significantly mitigate the effects caused by step activation signals.

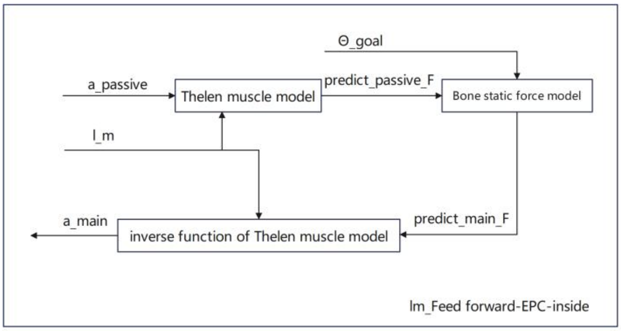

Fig. 10. FEPC Controller's internal structure(Picture credit : Original)

Fig. 10 shows the internal structure of the improved EPC controller. The output of EPC is no longer a fixed value but a variable that is dependent on the length under this control strategy. The deviation in muscle length can be integrated into the overall system deviation and managed by other controllers for to mitigate its effects. The control of the activation value output by the FEPC controller is illustrated in Fig. 11. Through this control method, the tremor issues caused by the control have been significantly reduced. The settling time has also decreased to some extent. Compared to the single EPC, the settling time of the FEPC has been reduced by approximately 10%, and the number of oscillations has decreased to just one.

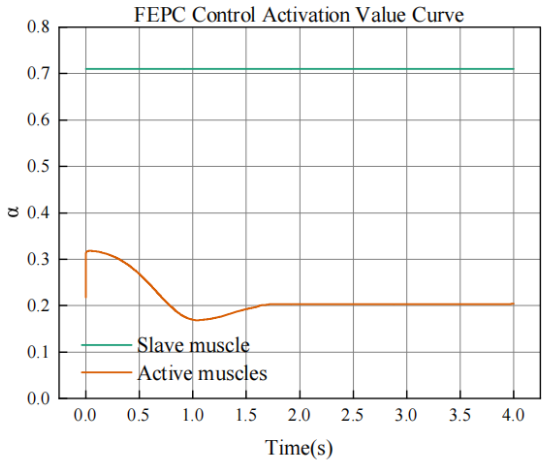

Fig. 11. The Improved EPC controller Control Curves(Picture credit : Original)

In order to mitigate the steady-state error of the FEPC, it is important to consider the potent changing activation values if a control algorithm is used concurrently with FEPC. The complex coupling could lead to instability in the control curves.

To solve this issue, fixing the EPC parameters is a solution: the controller's muscle length can be adjusted to a fixed final value when the steady-state error is less than the allowable correction error of the model. Then the EPC-GSC can be employed to reduce the steady-state error. This approach may still result in the same number of fluctuations but stabilizes more quickly. The control effect using this method is illustrated by the red curve in Fig. 12. From another perspective, after stabilizing the FEPC controller, the GSC can also be employed to reduce the steady-state error. This effectiveness of this control method is shown by the black curve in Fig. 12. Though this may increase the system's stabilization time, it allows for the significant reduction of fluctuations provided by the FEPC to be maintained. Therefore, if the model is established with sufficient accuracy and the deviations can be ignored, using FEPC as the main controller is a better improved control solution.

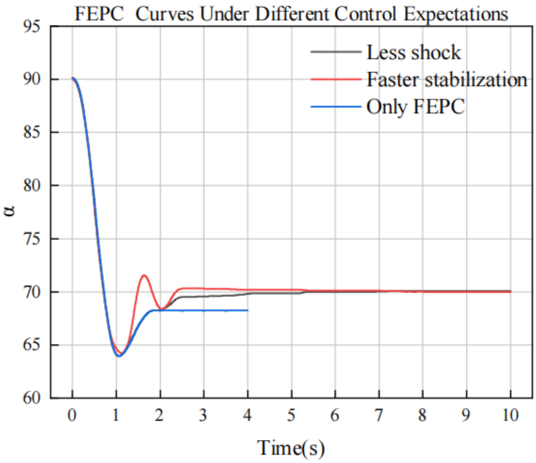

Fig. 12. Fig. 12 Control curves under the improved EPC-GSC controller.(Picture credit : Original)

4 Conclusion

This paper developed a detailed simulation model using the MuJoCo engine and general parameters from the literature, implementing traditional EPC-GSC control through this simulation model. To improve the stability of EPC control algorithm, the FEPC controller was proposed. From the results, although FEPC controller significantly outperforms the original scheme in terms of performance, the introduction of feedback has led to stability issues in the model, preventing the additional incorporation of GSC to reduce errors. Control can be separated through piecewise approach, but the segments for different postures are not consistent, which still presents certain limitations. Therefore, variable feedback tailored to specific models may become an effective approach for improving the EPC algorithm. Future research should focus on addressing the coupling stability issues between FEPC and control algorithm to achieve a more efficient and stable modified EPC control algorithm.

Reference

1. Zhang, J., et al.: 'Robotic artificial muscles: Current progress and future perspectives', IEEE Transactions on Robotics, 2019, 35, (3), pp. 761-781
2. Chou, C. P., Hannaford, B.: 'Measurement and modeling of McKibben pneumatic artificial muscles', IEEE Transactions on Robotics and Automation, 1996, 12, (1), pp. 90-102
3. Zhu, Y., Li, R., Song, Z.: 'Bionic muscle control with adaptive stiffness for bionic parallel mechanism', Journal of Bionic Engineering, 2023, 20, (2), pp. 598-611
4. Dai, Z., et al.: 'Design and Joint Position Control of Bionic Jumping Leg Driven by Pneumatic Artificial Muscles', Micromachines, 2022, 13, (6), pp. 827
5. Jia, Z., et al.: 'Design and Force/Angle Independent Control of a Bionic Mechanical Ankle Based on an Artificial Muscle Matrix', Biomimetics, 2024, 9, (1)

6. Gillespie, M. T., Best, C. M., Townsend, E. C., et al.: 'Learning nonlinear dynamic models of soft robots for model predictive control with neural networks', Proceedings of the 2018 IEEE International Conference on Soft Robotics (RoboSoft), IEEE, 2018, pp. 39-45
7. Wu, Y.: 'Analysis of anti-interference and motion control of musculoskeletal robots', PhD dissertation, University of Science and Technology Beijing, 2024. DOI: 10.26945/d.cnki.gbjku.2024.000017
8. Thelen, D. G.: 'Adjustment of muscle mechanics model parameters to simulate dynamic contractions in older adults', Journal of Biomechanical Engineering, 2003, 125, (1), pp. 70-77. DOI: 10.1115/1.1531112
9. Zajac, F. E.: 'Muscle and tendon: properties, models, scaling, and application to biomechanics and motor control', Critical Reviews in Biomedical Engineering, 1989, 17, (4), pp. 359-411
10. Shou, T.: 'Neurobiology', People's Health Publishing House, Beijing, 2001, (5th Edition).